PACKER ENGINEERING INC,
1950 North Washington Street,
Naperville, IL 60566

Metallurgical Evaluation of a DOT-3AA Cylinder, Serial No. 441106, with Pin Hole Leak

FINAL REPORT

June 2007

Prepared for
Mark Toughiry
Office of Hazardous Materials Technology
Pipeline and Hazardous
Materials Safety Administration
U.S. Department of Transportation

Purchase Order No. DTPH56-07-P-000007

Table of Contents

1.0 INTRODUCTION

Objective: - The purpose of this project is to determine chemical and metallurgical characteristics of the cylinder with a leak, initial point of fracture and possible cause of leak.

1.1 Technical Approach

In this project the DOT – 3AA cylinder with serial number 441106 was analyzed to determine the chemical and metallurgical characteristics of the leak.

The general condition of the cylinder was documented. The location of the leak was identified and documented. Radiography was performed on the cylinder to characterize and confirm the location of the leak. Ultrasonic inspection was performed to characterize the length of the crack and thickness of the cylinder near the crack. After performing the non-destructive testing, the cylinder was cut open. The inside surface of the cylinder was documented. Chemical analysis was performed on a sample removed from the cylinder. Magnetic particle testing was performed on the identified leak location to confirm the size of the crack. The cylinder was cut open to perform fractographic analysis on the leak surface. The fracture surface was documented using a stereomicroscope, before cleaning the oxide scale. An Energy Dispersive Spectroscopy (EDS) analysis was performed on the uncleaned fracture surface. The fracture surface was cleaned using ultrasonic cleaning and replica strip cleaning technique. The cleaned fracture surface was analyzed using the scanning electron microscope. After completing the fractographic analysis the sample was cut perpendicular to the fracture surface and the microstructure was analyzed and compared to the microstructure of the sample cut in the same grain direction but away from the fracture surface. Microhardness was measured on both samples. Rockwell hardness was measured along the length of the largest piece of the cylinder using ASTM E-18-98. A tensile test was performed to measure the strength and ductility of the ruptured cylinder in accordance with 49 CFR 178.37- K and L.

2.0 GENERAL DOCUMENTATION OF THE CYLINDER

2.1 Visual Documentation and Cylinder Specifications

The cylinder was identified as a DOT - 3AA cylinder with serial number 441106 as shown in Figure 1. The indented markings on the cylinder are as shown in Figure 2.

- The cylinder is marked as DOT – XXXXXXX GL Limited 441106. 119501 6 A 06 TP377 5PSI 11566 VA3.3.
- As per the information provided to Packer Engineering Inc by DOT, the service pressure of the cylinder is 2,265 psi. The minimum design wall thickness is 0.228 inch.
- The maximum diameter of the cylinder is 9 inches as measured by Packer Engineering Inc.
- The surface of the cylinder appears to be sandblasted.
- A surface flaw was observed in the transverse direction of the cylinder as shown in Figure 3. It is located 16.5 inches from the bottom of the cylinder. A higher magnification image of the surface flaw is as shown in Figure 4.

2.2 Non Destructive Evaluation

X-ray radiography was performed on the cylinder to characterize the surface flaw on the cylinder. The cylinder was radiographed in two different orientations. The first orientation consisted of a longitudinal view of the cylinder with the source perpendicular to the outer surface at the flaw location. The radiograph in Figure 5 indicates that it is not simply a surface flaw, but that the flaw penetrates a significant portion of the cylinder wall. The second orientation was in the transverse direction with the source at a 45 degree angle to the defect. The radiograph in Figure 6 also shows the defect and confirms that it is not just a surface flaw.

Pressure testing was performed on the cylinder using air to confirm the presence of the leak. The cylinder was connected to a portable air compressor with a test gauge and regulator in-line between the compressor and the cylinder. Gas Leak Detector (soap solution) was applied on the cylinder surface and pressure was slowly applied. At approximately 5 psi, bubbles were visible from the area of the surface flaw. The test was continued up to approximately 20 psi, at which air could be felt escaping through the flaw. No other leak was detected in the cylinder. This test was repeated two times to confirm the findings.

Ultrasonic inspection was performed to analyze the leak and thickness variation of the cylinder along the length. Figure 7 shows the ultrasonic testing of the cylinder. The shear wave analysis at the leak using 5mHz, 45º shoe, ½" diameter from 180 º back indicates the depth of the crack is 0.158 inch as indicated by Figure 8. The maximum depth of the crack is 0.174 inch as shown in Figure 9. The maximum length of the crack determined by ultrasonic inspection was 0.63 inch. The thickness of the cylinder was analyzed using

shear wave around the circumference of the cylinder containing the crack. Table I lists the thickness measurements along the cylinder length in the plane that contains the leak. The wall thickness 3 inches above the bottom of the cylinder is 0.242 inch. The wall thickness near the crack is 0.244 inch. These thickness measurements indicate that the wall thickness of the subject cylinder meets the 0.228 inch minimum design requirement.

TABLE I
Thickness measurement along the length of the cylinder

#	Distance of the cylinder from bottom (inch)	Thickness along the length of cylinder and in the plane containing leak (inch)
1	3	0.242
2	12	0.243
3	16	0.244
4	24	0.246
5	36	0.253
6	46	0.255

3. METALLURGICAL ANALYSIS

3.1 Visual Observation and Sectioning of the Cylinder

Figure 10 shows the location at which the cylinder was sectioned. Figure 11 indicates the presence of corrosion products on the inside wall of the cylinder. The inside surface at the leak is as shown in Figure 12. The samples for tensile testing and chemical analysis were sectioned from the area marked in Figure 13 and Figure 14. The arrows shown in the Figure 13 and Figure 14 indicate the leak location. The cylinder was sectioned as shown in Figure 15 to cut open the leak. Fractography and metallograhy were performed on one surface of the leak and the other side of the leak was retained.

3.2 Chemical Analysis of the Cylinder

The chemical analysis of the subject DOT-3AA cylinder with serial number 441106 was compared to the steel materials authorized for DOT-3AA cylinders by the Code of Federal Regulations (CFR) 49, Chapter I – Research and Special Programs Administration, Department of Transportation, Subchapter C- Hazardous Material Regulations, part § 178.37. The comparison is as shown in Table II. The composition of the subject DOT-3AA cylinder meets the specifications for 4130X steel.

TABLE II
Comparison of the chemistry of the subject DOT cylinder with steel authorized for DOT-3AA cylinder as per 49 CFR part § 178.37

Elements	Designation						
	Subject DOT cylinder (%)	4130X (%)	NE8630 (%)	9115 (%)	9125 (%)	Carbon-Boron (%)	Intermediate Manganese (%)
Carbon	0.31	0.25/0.35	0.28/0.33	0.10/0.20	0.20/0.30	0.25- 0.37	0.40 max
Manganese	0.58	0.40/0.90	0.70/0.90	0.50/0.75	0.50/0.75	0.80-1.40	1.35/1.65
Phosphorus	0.011	0.04 max	0.04 max	0.04 max	0.04 max	0.035 max	0.04 max
Sulfur	0.008	0.05 max	0.04 max	0.04 max	0.04 max	0.045 max	0.05 max
Silicon	0.27	0.15/0.35	0.20/0.35	0.60/0.90	0.60/0.90	0.3 max	0.10/0.30
Chromium	0.84	0.80/1.10	0.40/0.60	0.50/0.65	0.50/0.65	-	-
Molybdenum	0.17	0.15/0.25	0.15/0.25	-	-	-	-
Zirconium	-	-	-	0.05/0.15	0.05/0.15	-	-
Nickel	0.02	-	0.40/0.70	-	-	-	-
Boron	-	-	-	-	-	0.005/0.003	-
Copper	0.03	-	-	-	-	-	-
Aluminum	0.04	-	-	-	-	-	-

3.3 Fractography and Metallography

The cut section of the cylinder was observed under stereomicroscope at up to 60 X magnification. Figures 16 -18 show the stereoscope images of the section containing fracture. The surface of the as-received fracture appears to be corroded as indicated in Figure 18. The EDS analysis of the as-received fracture surface is shown in Figure 19. It indicates presence of iron (Fe), chromium (Cr), silicon (Si), carbon (C) oxygen (O), sulfur (S), silicon (Si), aluminum (Al), copper (Cu), chlorine (Cl), nickel (Ni) and sodium (Na). The fracture surface was then cleaned using replica strip cleaning, ultrasonic cleaning and rinsing with acetone. Even after cleaning several times, the fracture surface had an adherent oxide layer. The cleaned fracture surface was observed using scanning electron microscopy (SEM). Figures 20-22 show the fracture surface at the ID, center and OD of the cylinder wall respectively. As seen in the figures, the details of the fracture are obscured by oxides.

In order to perform metallographic analysis, the section containing fracture surface (Sample A) was cut perpendicular to the fracture and compared to the microstructure of the sample cut in the same grain direction but away from the fracture surface (Sample B). The metallurgical mounts were prepared by polishing and etching with 2% Nital solution.

Sample A (containing fracture surface):
The micrographs across the fracture surface can be seen in Figures 23 to 29. Figure 24 indicates presence of oxide layer on the fracture surface and also indicates presence of copper-colored phase. Figure 30 shows that the overall microstructure across the cylinder wall is tempered martensite. However, the microstructure at the periphery of both OD and ID of the cylinder wall indicates decarburization in some areas as seen in Figures 31 and 32 respectively. Two crack-like areas can be seen at the OD of the cylinder wall as shown in Figure 31. They are non-propagating and not related to the fracture of the cylinder.

Sample B (away from fracture surface):
The overall microstructure of the sample taken away from fracture surface is also tempered martensite as shown in Figure 33. Also there was decarburization observed at the ID of the sample as shown in Figure 34.

An EDS analysis was performed to evaluate the composition of the copper-colored phase and the dark and light gray oxide layer. Three areas at the fracture surface were analyzed as shown in Figure 35. The EDS at Location 1 and 2 and 3 are shown in Figure 36, 37 and 38, respectively. EDS at Location 1 indicates presence of copper (Cu), aluminum (Al), tin (Sn) and iron (Fe). The EDS at Location 2 (dark gray) shows presence of iron (Fe), chromium (Cr), silicon (Si), sulfur (S), chlorine (Cl), copper (Cu) and oxygen (O). The EDS at Location 3 (light gray) indicates that iron (Fe), manganese (Mn) and oxygen (O) are present.

4 MECHANICAL PROPERTY EVALUATION

4.1 Tensile Test

Tensile sample was obtained from the location as shown in Figure 13. The testing was performed in accordance with 49 CFR 178.37-K and L. The results are as shown in Table III. The tensile properties of the subject DOT-3AA cylinder were compared to the mechanical properties of 4130 steel at tempering temperatures of 1000 ºF and 1200 ºF [2]. Part 178.37 of 49 CFR (g) (4) indicates that the minimum tempering temperature may not be less than 1000 ºF. Hence, the tensile test results were compared to only the values listed at 1000 ºF and above. As seen in the table, the tensile properties of the subject DOT-3AA meet the specifications as notes above.

TABLE III
Tensile test results of DOT-3AA cylinder compared to the tensile properties of 4130 steel

Property	**DOT-3AA cylinder**	**4130 Steel (Tempered at 1000 ºF) [ref 2]**	**4130 Steel (Tempered at 1200 ºF) [ref 2]**
Tensile Strength	125 ksi	150 ksi	118 ksi
Yield Strength (0.2% offset)	110 ksi	132 ksi	102 ksi
% Elongation in 2 inches	20%	17%	22%

4.2 Rockwell Hardness Test

The Rockwell Hardness Test was performed along the largest piece of the cylinder in accordance with ASTM E18-98. The hardness tester was calibrated using a Patriot Manufacturing Company standard block with serial number 00B5167 and standard hardness value of 32.3 +/- 1.0 HRC. The hardness measured using the standard block was 33.2 at the beginning of the test and 32.0 at the end of the test. The results are as shown in Table IV. The hardness values of 4130 steel at tempering temperatures of 1000 ºF and 1200 ºF are 34 HRC and 24 HRC respectively [2]. The hardness of the DOT-3AA cylinder indicates that it was tempered above 1000 ºF.

Table IV
Rockwell hardness results of the DOT-3AA cylinder compared to the hardness values of 4130 steel

Location	**DOT-3AA cylinder (HRC)**	**4130 Steel (Tempered at 1000 ºF) (HRC) [ref 2]**	**4130 Steel (Tempered at 1200 ºF) (HRC) [ref 2]**
1	28	34	24
2	27		
3	26		
4	27		
5	27		
6	26		

4.3 Microhardness Evaluation

The microhardness was evaluated for the metallurgical mounts prepared across the fracture surface and away from the fracture using ASTM E92 - 03. The results are indicated in Table V and Table VI. The average hardness at about the center of the cylinder wall thickness is similar for both samples. However, the average hardness at the OD and ID is closer to the fracture surface, which is most likely due to decarburization.

TABLE V
Hardness measurements close to the fracture surface

#	Distance From OD (inches)	Hardness (HRC)	Average (HRC)
1	0.007 (Close to OD)	22	21
2	0.014 (Close to OD)	21	
3	0.021 (Close to OD)	21	
4	0.112 (center)	26	25
5	0.119 (center)	25	
6	0.126 (center)	24	
7	0.217 (Close to ID)	19	21
8	0.224 (Close to ID)	22	
9	0.231 (Close to ID)	22	

TABLE VI
Hardness measurements away from fracture surface

#	Distance From OD (inches)	Hardness (HRC)	Average (HRC)
1	0.007 (Close to OD)	26	26
2	0.014 (Close to OD)	26	
3	0.021 (Close to OD)	27	
4	0.112 (center)	25	26
5	0.119 (center)	26	
6	0.126 (center)	27	
7	0.217 (Close to ID)	22	25
8	0.224 (Close to ID)	26	
9	0.231 (Close to ID)	27	

5 DISCUSSION

Metallurgical evaluation was performed on the DOT - 3AA cylinder with serial number 441106 to identify the cause and origin of the leak. The leak was located 16.5 inches from the bottom of the cylinder. The presence of a leak was confirmed using non-destructive techniques such as radiography, pressure testing and ultrasonic testing. The leak was oriented in the transverse direction. Hence, hoop stresses created by internal gas pressure cannot be responsible for the rupture.

The composition of the DOT - 3AA cylinder meets the specifications for 4130X steel as given in 49 CFR, part § 178.37. The tensile strength, yield strength, elongation and hardness of the DOT - 3AA cylinder indicate it was tempered above 1000^{o}F as required in 49 CFR, part § 178.37 (g) – 4.

Metallography and EDS of the fracture surface showed that a copper-rich phase containing a small amount of tin is present along the grain boundaries near the fracture and in the oxide on the fracture surface. The copper-tin phase most likely represents the remnants of a bronze-type material that came into contact with the cylinder while the cylinder was near its hot deformation temperature. The bronze material melted and was included into the steel. Based on the presence of copper and tin, and the apparent lack of elements such as zinc, aluminum, nickel and lead, it may be speculated that a phosphor bronze material contacted the cylinder. However, the precise identification of the copper-bearing material is not significant for determination of the process by which the leak formed in the subject cylinder.

If the bronze material entered the molten 4130X alloy, the bronze would likely have dissolved and become distributed throughout the billet. However, the nominal copper content of the cylinder was determined to be 0.03%. Bulk copper concentration at 0.03% would not be considered to be elevated, or high enough to cause cracking. Finally, copper-rich phases in grain boundaries were not seen in the microstructure away from the fracture. Therefore, the bronze material most probably did not enter the molten steel alloy.

The recommended temperatures for hot deformation processes such as forging or extrusion generally range from 1600^{o}F to 2245^{o}F for 4130 [3]. The liquidus temperature for phosphor bronze alloys generally ranges from 1800-1920^{o}F (The liquidus for pure copper is 1950^{o}F.) [4]. Note that the recommended austenitizing temperature for 4130 is 1600^{o}F which would be too low to melt bronze or pure copper. Therefore, the inclusion of the copper alloy into the cylinder must have occurred during hot deformation. Based on the observation that the crack was wider at the OD of the wall compared with the ID, it is likely that the crack was initiated by inclusion of copper at the OD and propagated toward the ID.

The thick oxide layers on the fracture surface of the leak indicate the crack was open during hot deformation and subsequent heat treatment. The presence of copper phases in

the oxide layers indicates the bronze component was molten as the oxide films were forming during hot deformation.

Cracking of steel resulting from contact with molten bronze has been reported in locomotive axles when bearing failure resulted in frictional heating of bronze bearing components to the point where molten bronze contacted the steel axle. This phenomenon has been characterized as liquid metal embrittlement. Three factors are generally required for embrittlement of steel by copper: (1) applied tensile stress, (2) wetting of the steel by molten copper, and (3) heating the steel into the austenite range [5]. In the case of the DOT cylinder, tensile stress would have been created during hot deformation. Note that the transverse orientation of the leak would be consistent with the direction of tensile stresses created during deformation to form the cylinder. Also, the requirement that a tensile stress be present suggests that the bronze came into contact with the billet prior to forging rather than after forging was complete and stresses were thermally relieved. Wetting by copper would have occurred when the bronze material contacted the steel at forging temperature and the steel would have been in the austenite range at forging temperature. Therefore, the commonly recognized requirements for liquid metal embrittlement were present when the DOT – 3AA cylinder was formed.

6 CONCLUSIONS

The leak on the DOT – 3AA cylinder was caused by liquid metal embrittlement. A localized area of the cylinder was liquid metal embrittled by contact with a copper-rich material, probably a phosphor bronze, while the cylinder was at forging temperature.

This concludes the metallurgical evaluation of a DOT-3AA cylinder with serial no. 441106 with pin hole leak. If you have questions or need additional information please email us at mpareek@packereng.com or call at 630-577-1930.

Sincerely,

PACKER ENGINEERING, INC.

Mridula L Pareek
Engineering Technologist

Craig L. Jensen, Ph.D., P.E.
Materials Engineering, Director

7 FIGURES

Figure 1: DOT-3AA cylinder as received

Figure 2: Indented marking on the DOT-3AA cylinder

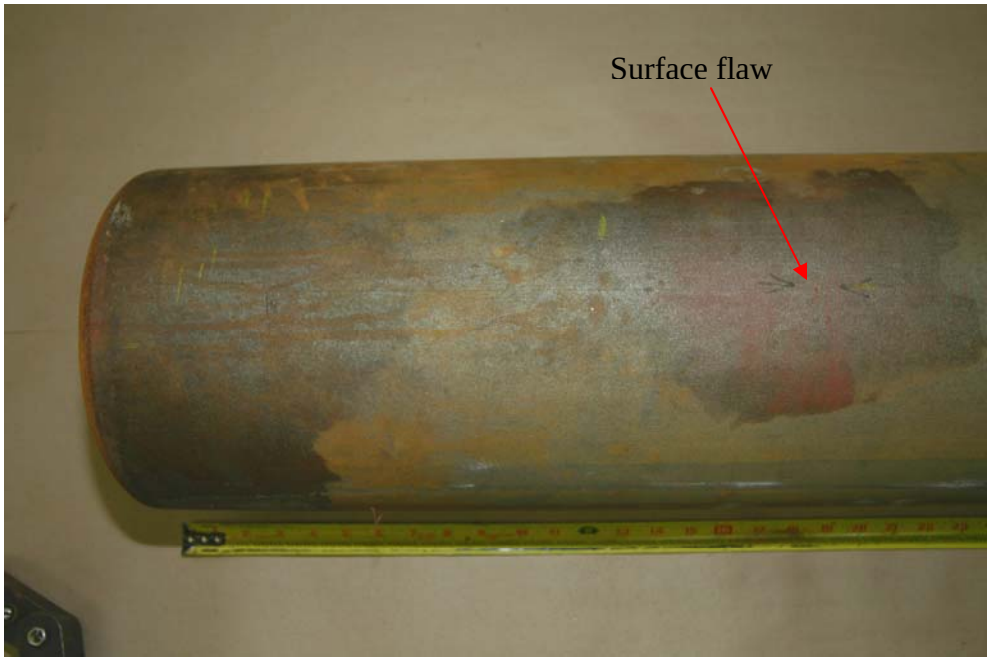

Figure 3: Surface flaw in the transverse direction on the DOT-3AA cylinder

Figure 4: Surface flaw on the DOT-3AA cylinder

Figure 5: Radiograph of DOT cylinder with the X-ray source perpendicular to the flaw. The arrow is pointing to the defect.

Figure 6: Radiograph of DOT cylinder with X-ray source at 45 º to the flaw. The arrow is pointing to the defect.

Figure 7: Ultrasonic testing of the DOT-3AA cylinder

Figure 8: Ultrasonic testing - crack depth from 180 º back measured using shear wave analysis

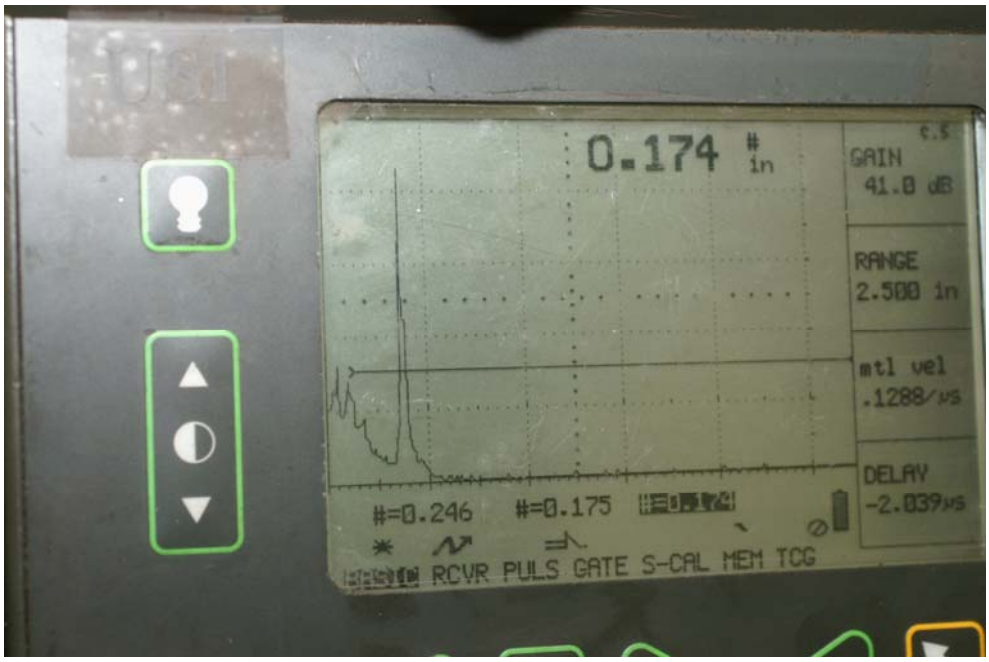

Figure 9: Ultrasonic Testing - maximum depth of crack measured using shear wave analysis

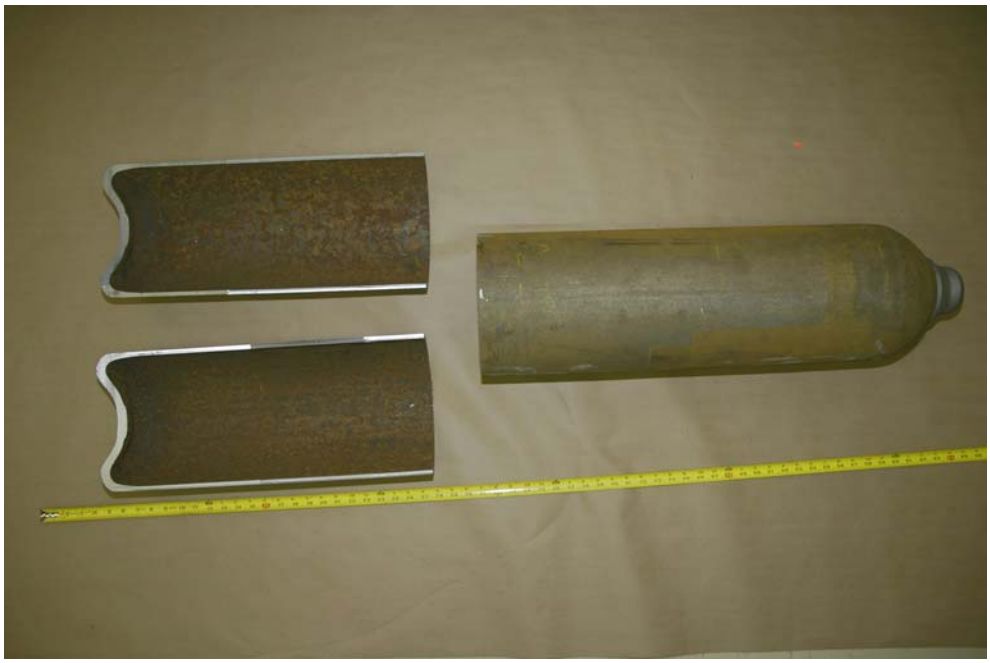

Figure 10: Showing location of sectioning of the DOT-3AA cylinder

Figure 11: Shows corrosion on the inside wall of the cylinder

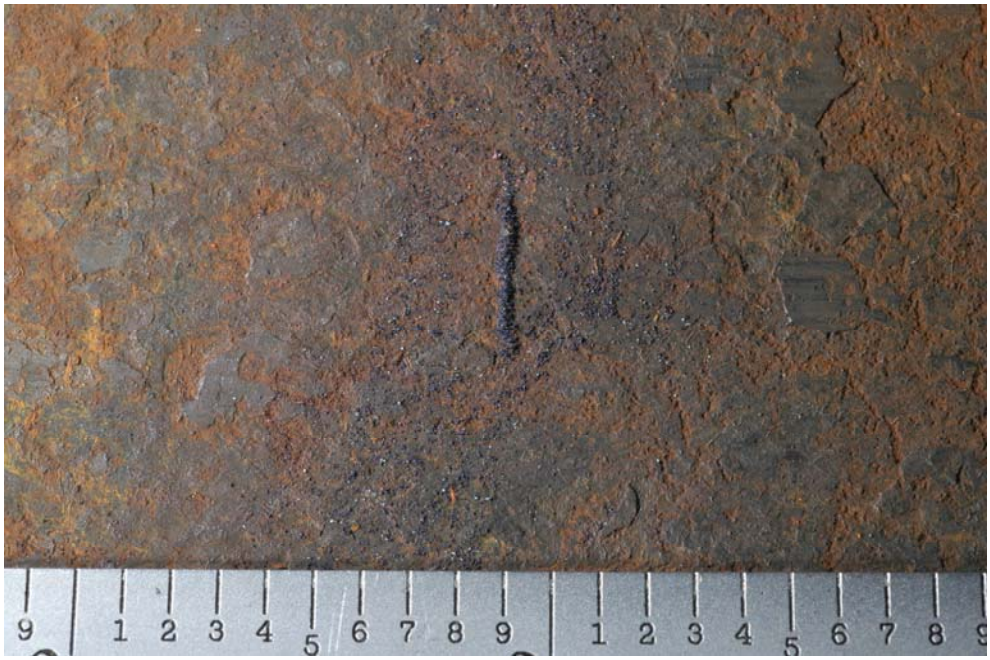

Figure 12: Shows the inside surface of the leak

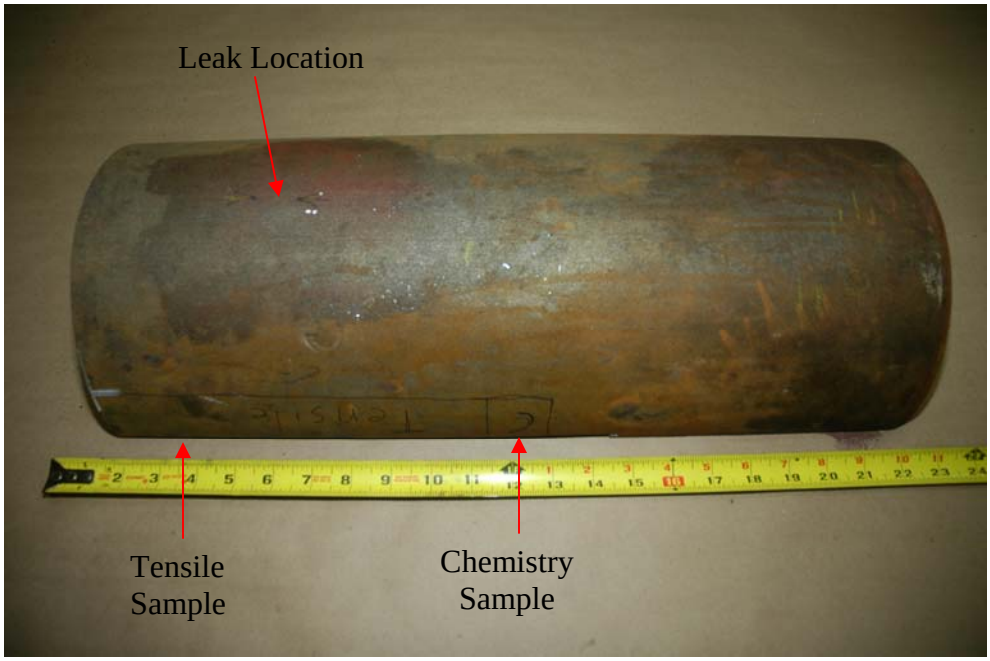

Figure 13: Shows location at with the samples for tensile testing and chemistry analysis were sectioned

Figure 14: Shows sections cut for tensile testing and chemistry analysis.

Figure 15: Sectioning of the cylinder to cut open the leak

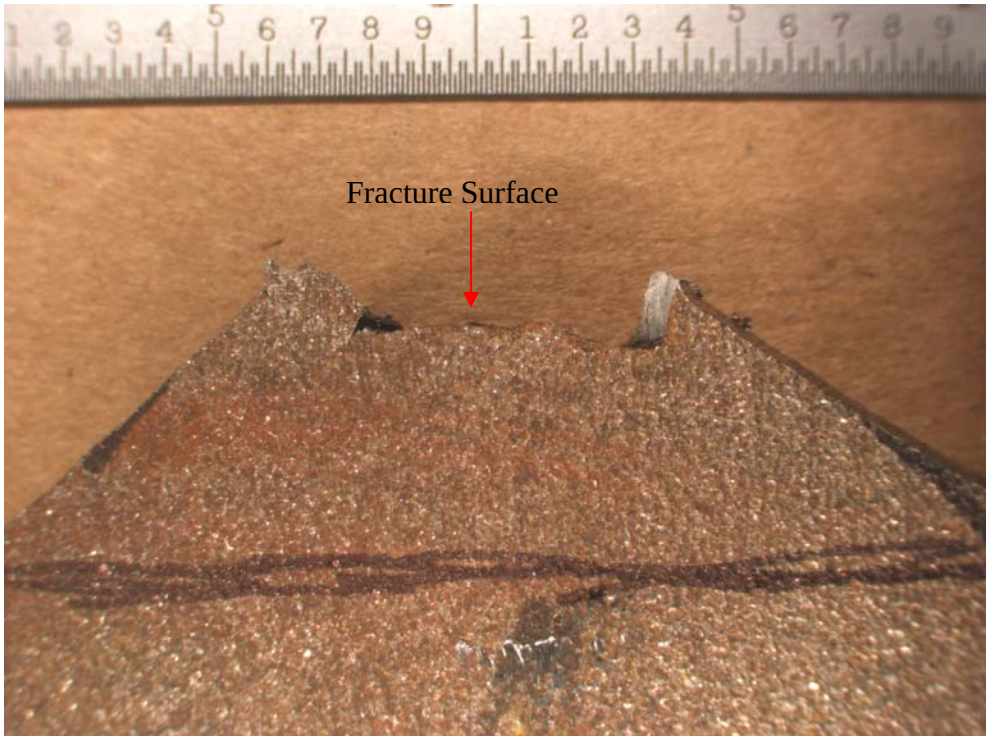

Figure 16: Seteroscope image of the outer surface of the cylinder section containing the fracture surface. Magnification 65X

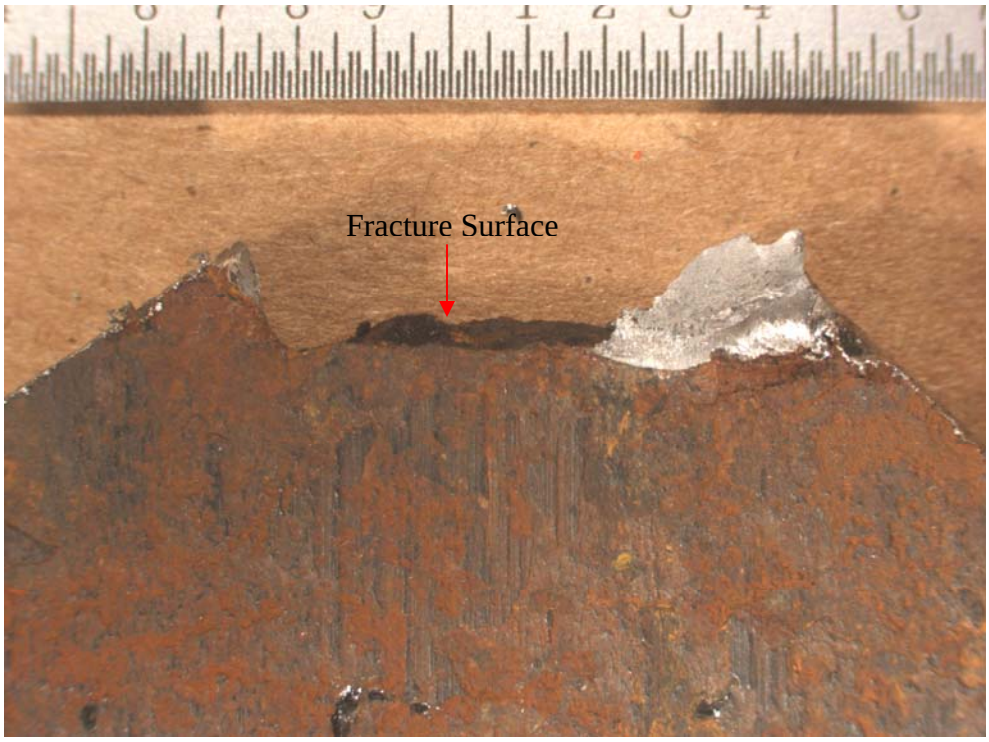

Figure 17: Stereoscope image of the inner surface of the cylinder section containing the fracture surface. Magnification 65X

Figure 18: Stereoscope image of the cylinder section showing the fracture surface. Magnification 65X

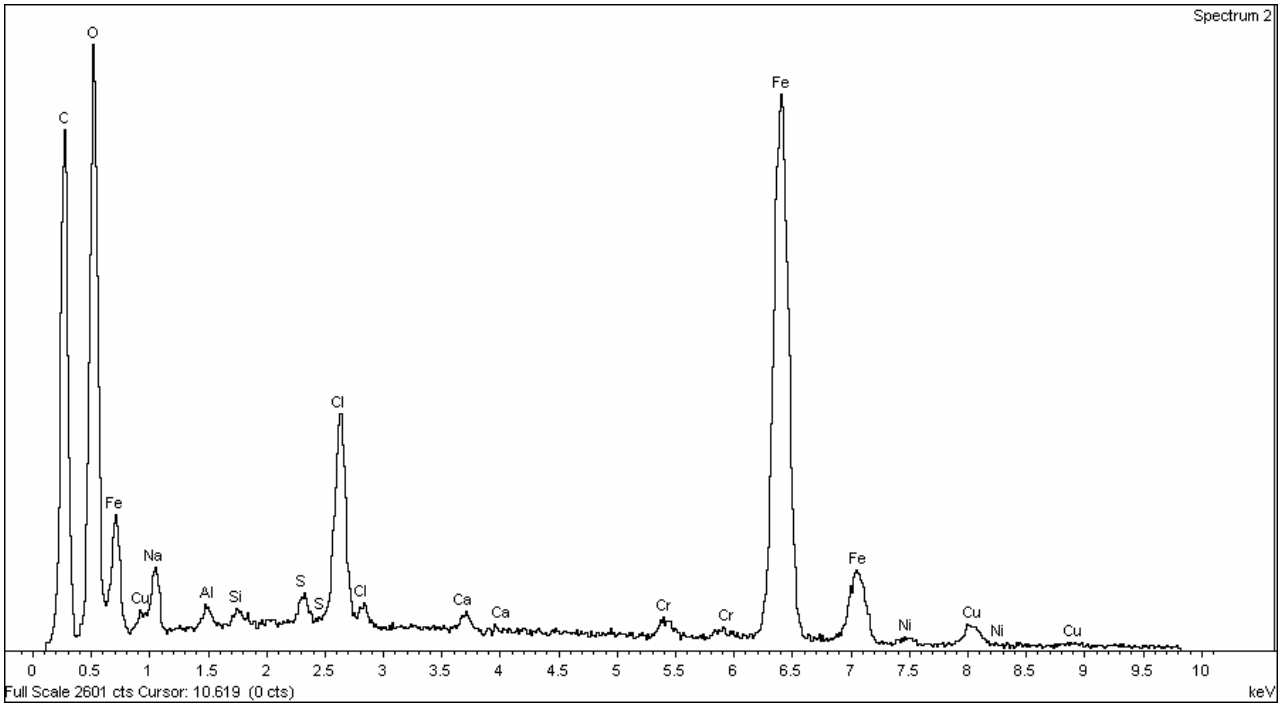

Figure 19: EDS of the non-cleaned fracture surface of the cylinder

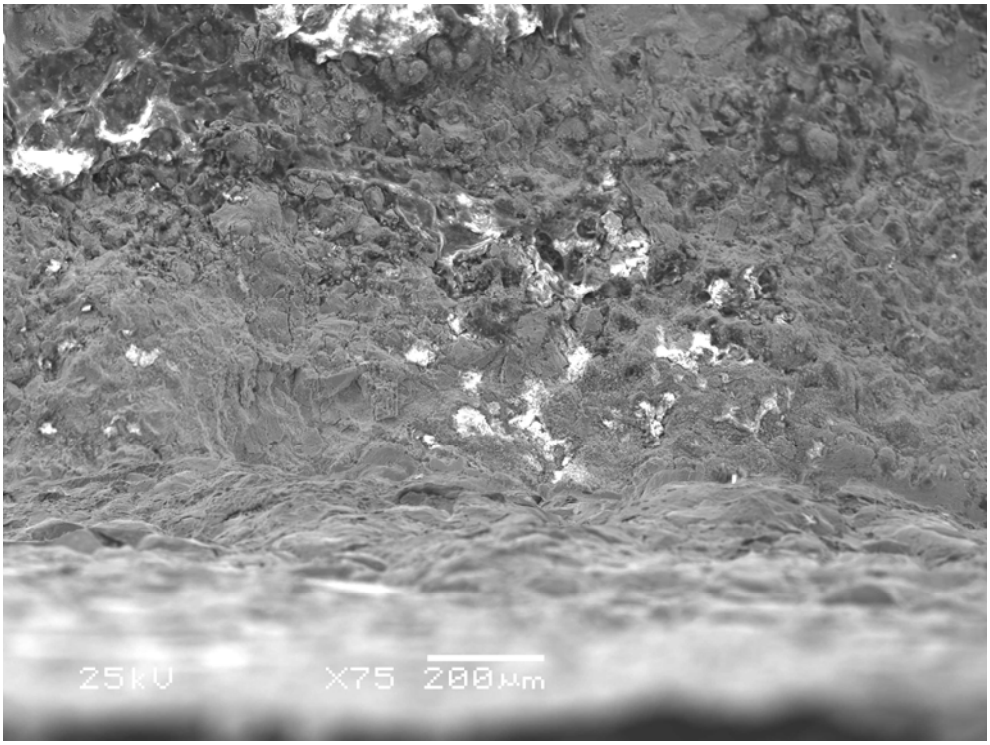

Figure 20: SEM image of the fracture surface close to the inner diameter of the cylinder wall. Magnification 75X.

Figure 21: SEM image at the center of the fracture surface. Magnification 75X

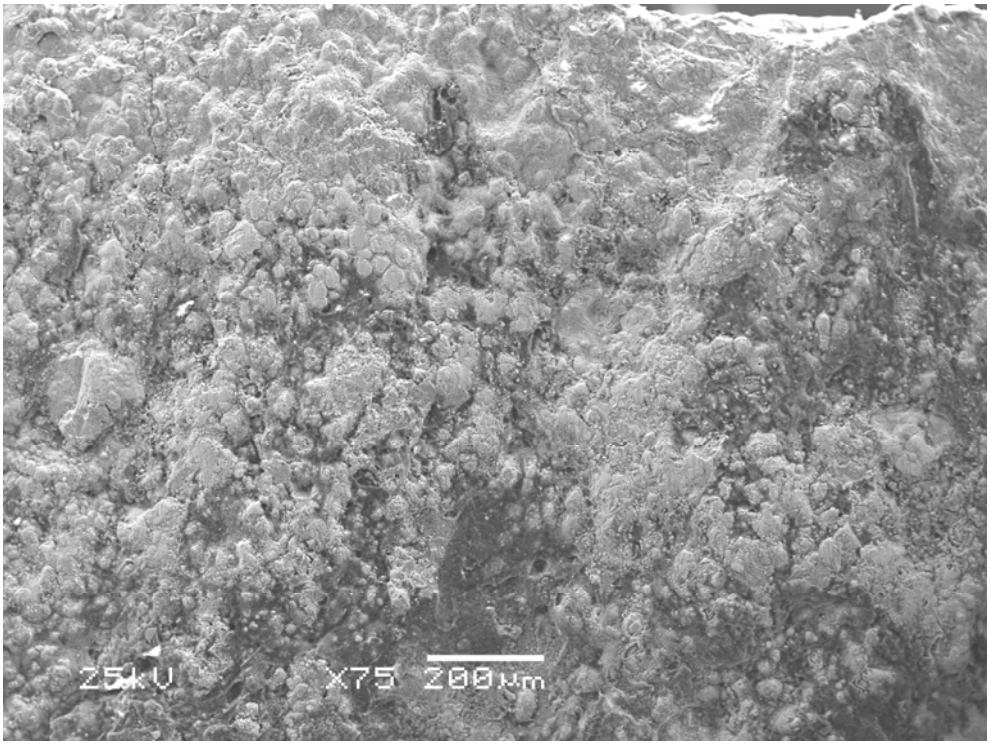

Figure 22: SEM image of the fracture surface close to the outer diameter of the cylinder wall. Magnification 75 X

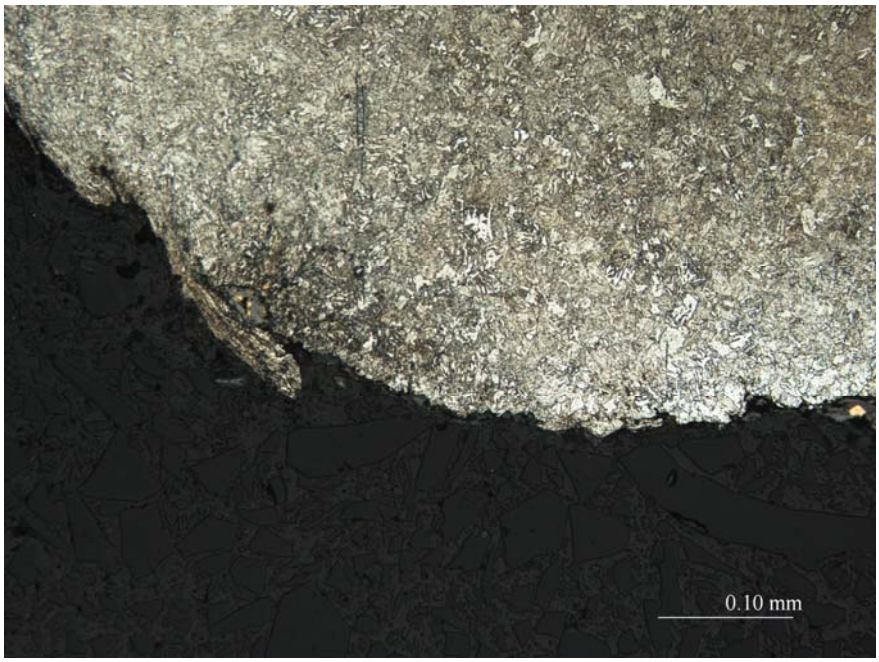

Figure 23: Microstructure across the fracture surface at the outer diameter of the cylinder. Magnification 200X. Etchant: 2% Nital

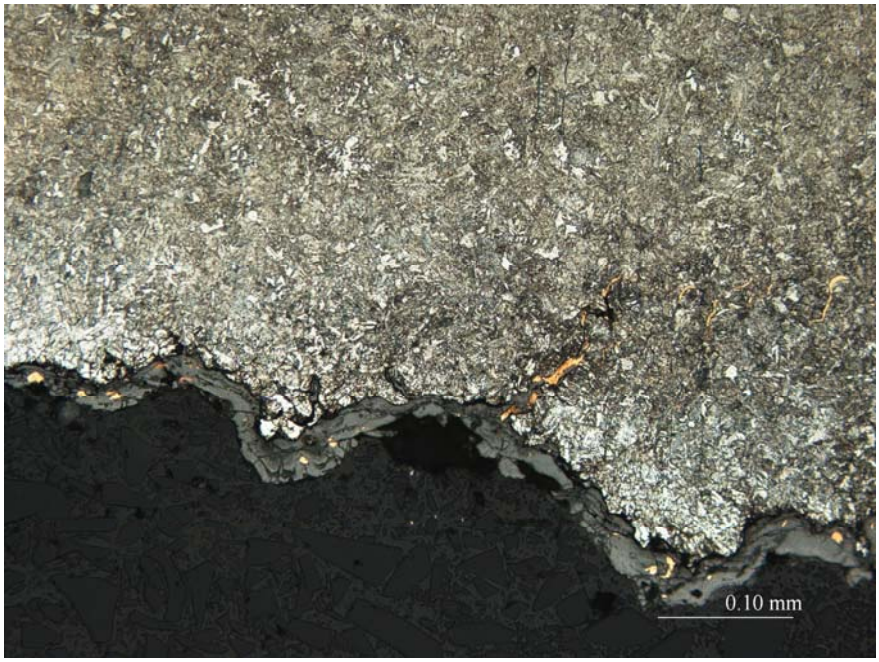

Figure 24: Microstructure across the fracture surface showing tempered martensite structure, presence of corrosion products (gray) and copper colored phase (orange) in continuation with Figure 23. Magnification 200X. Etchant: 2% Nital

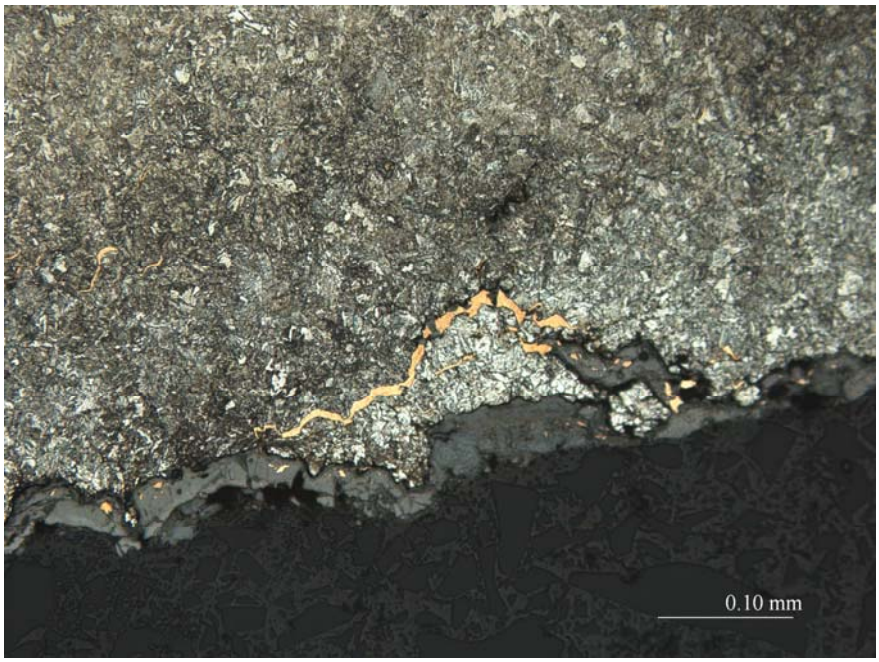

Figure 25: Microstructure across the fracture surface showing copper colored phase in the tempered martensite structure in continuation with Figure 24. Magnification 200X. Etchant: 2% Nital

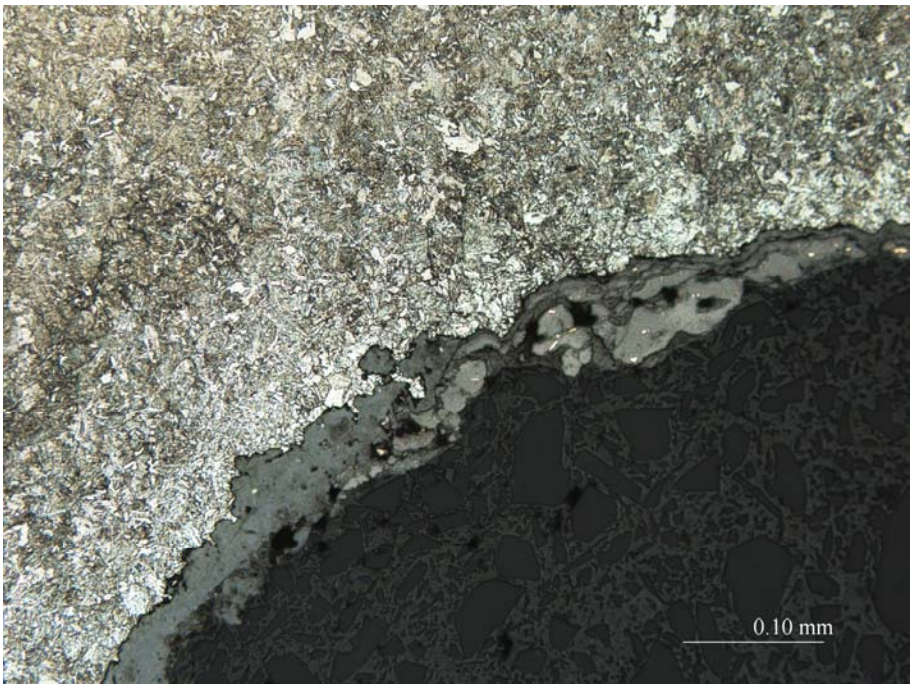

Figure 26: Microstructure across the fracture surface in continuation with Figure 25. Magnification 200X. Etchant: 2% Nital

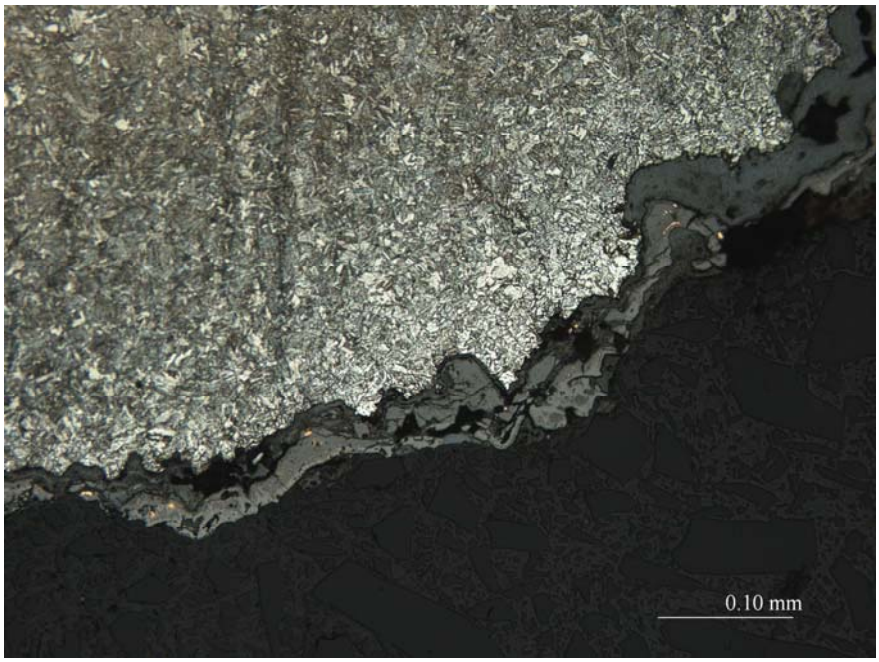

Figure 27: Microstructure across the fracture surface in continuation with Figure 26. Magnification 200X. Etchant: 2% Nital

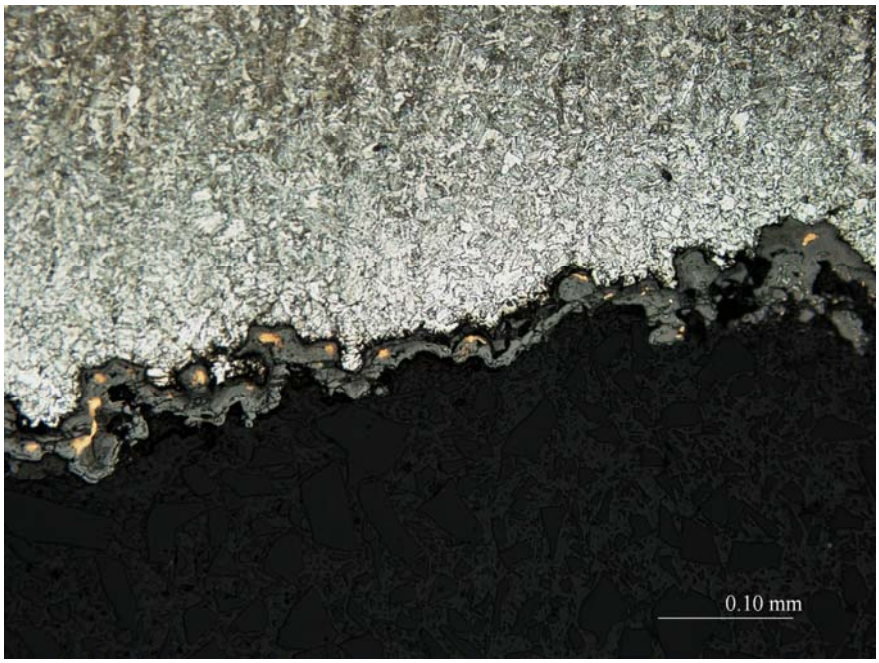

Figure 28: Microstructure across the fracture surface in continuation with Figure 26. Magnification 200X. Etchant: 2% Nital

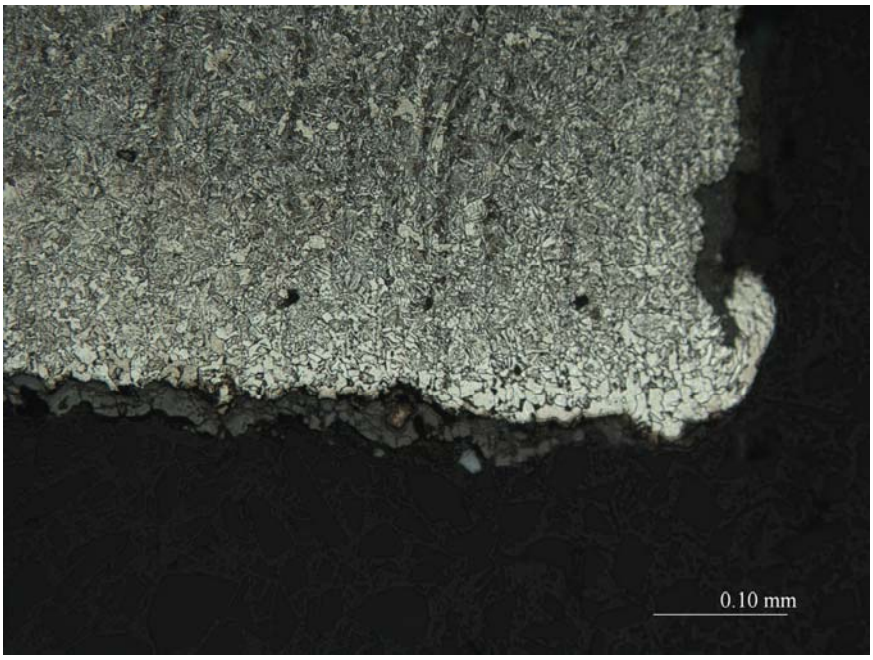

Figure 29: Microstructure across the fracture surface at the ID in continuation with Figure 28. Magnification 200X. Etchant: 2% Nital

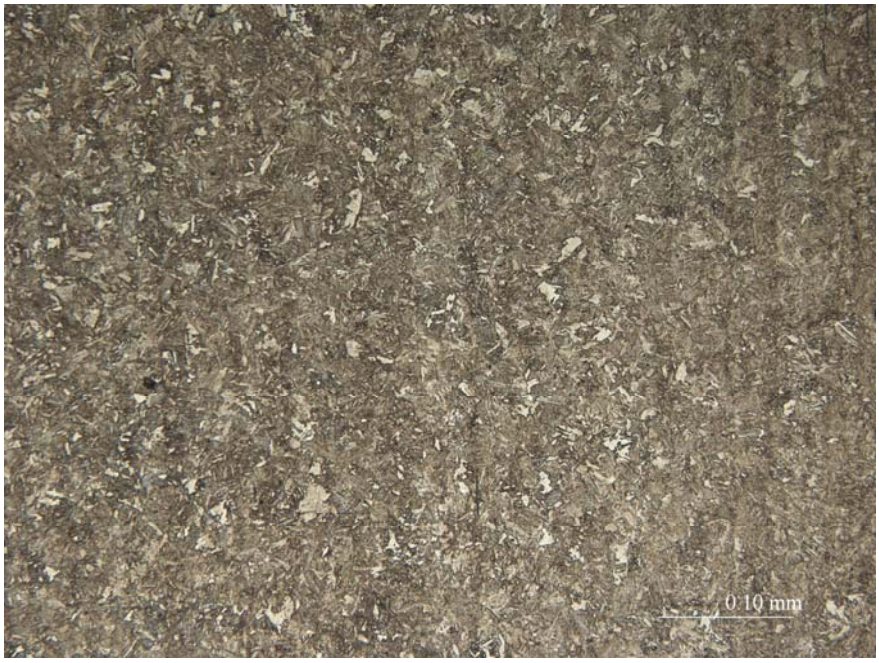

Figure 30: Tempered martensite structure observed in the sample containing fracture surface. Magnification 200X. Etchant: 2% Nital

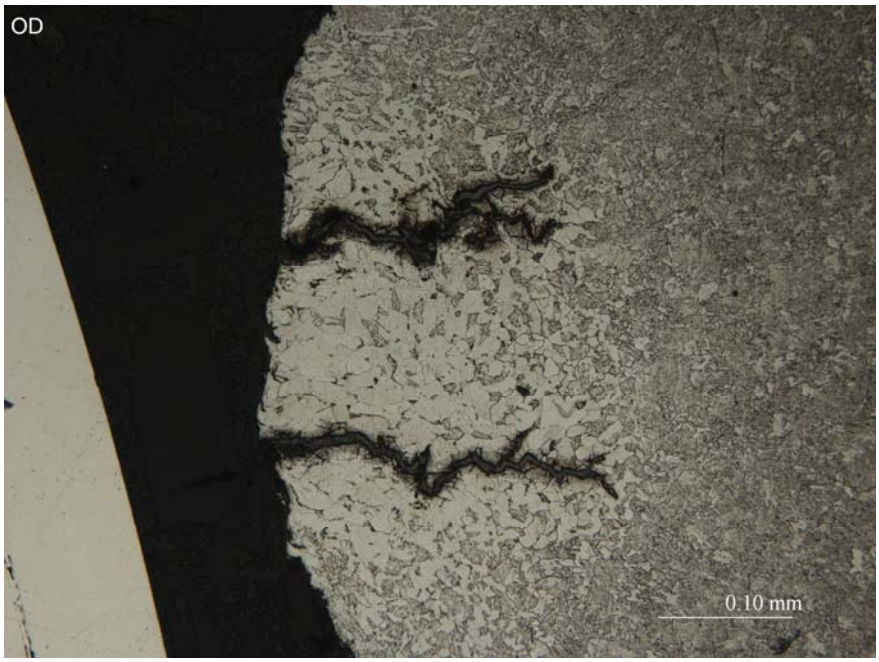

Figure 31: Shows decarburization at the OD of the cylinder in the sample containing fracture surface. Two crack like areas can be seen in the decarburized region. Magnification 200X. Etchant: 2% Nital

Figure 32: Shows decarburization at the ID of the cylinder in the sample containing fracture surface. Magnification 200X. Etchant: 2% Nital

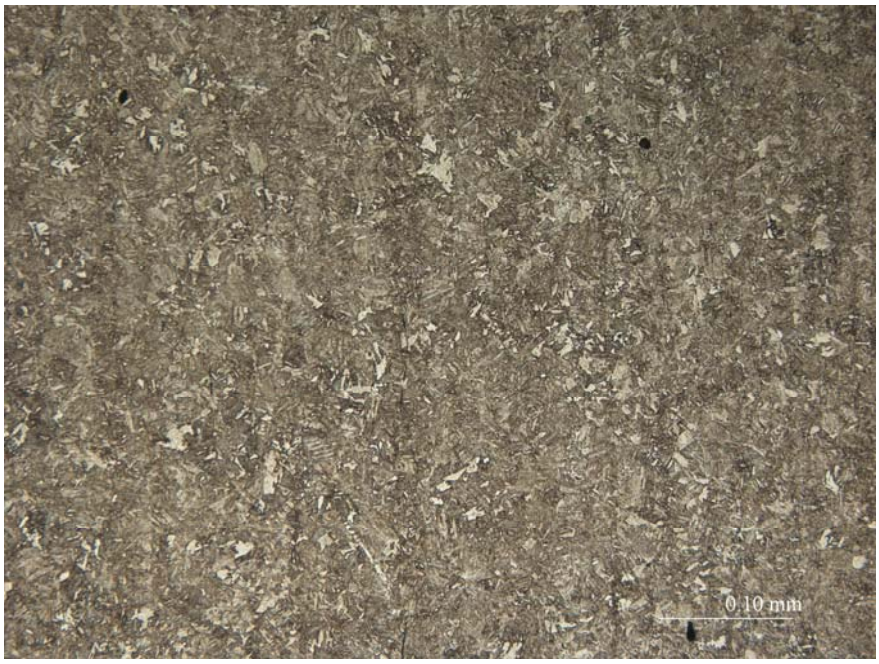

Figure 33: Tempered martensite structure observed in the sample taken away from the fracture surface. Magnification 200X. Etchant: 2% Nital

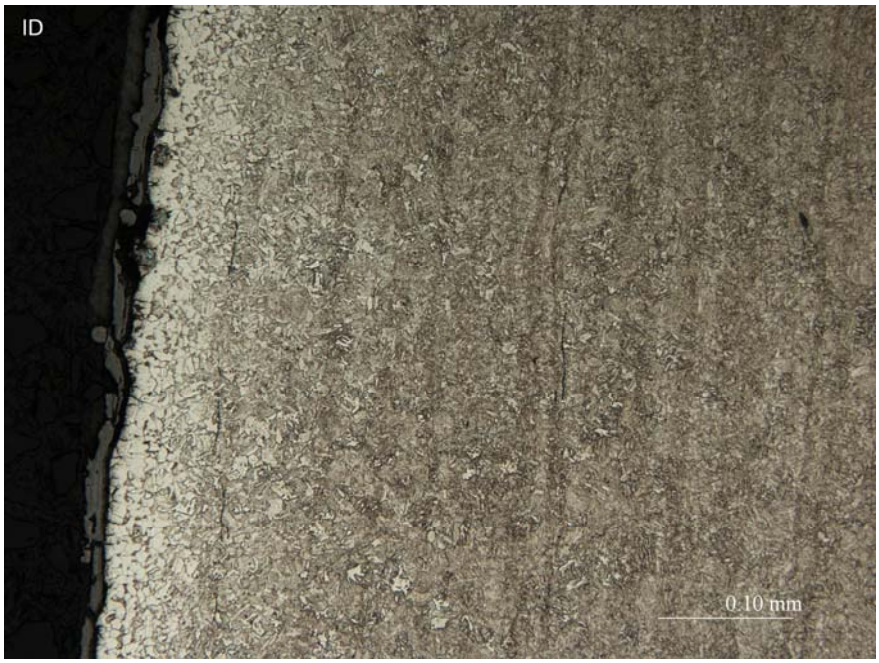

Figure 34: Shows decarburization at the ID of the sample taken away from the fracture surface. Magnification 200X. Etchant: 2% Nital

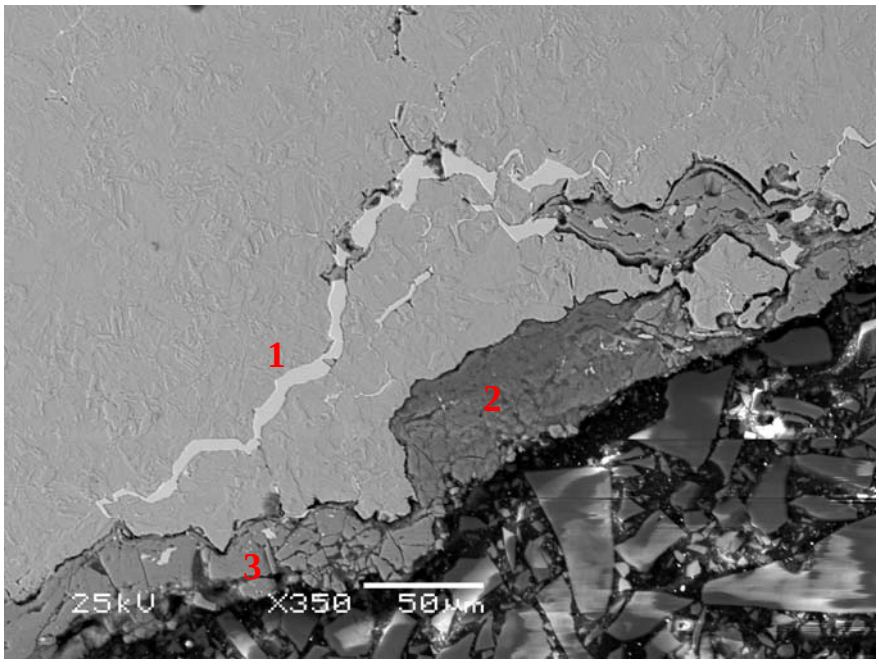

Figure 35: Shows the locations near the fracture surface at which EDS analysis was performed. Magnification 350X.

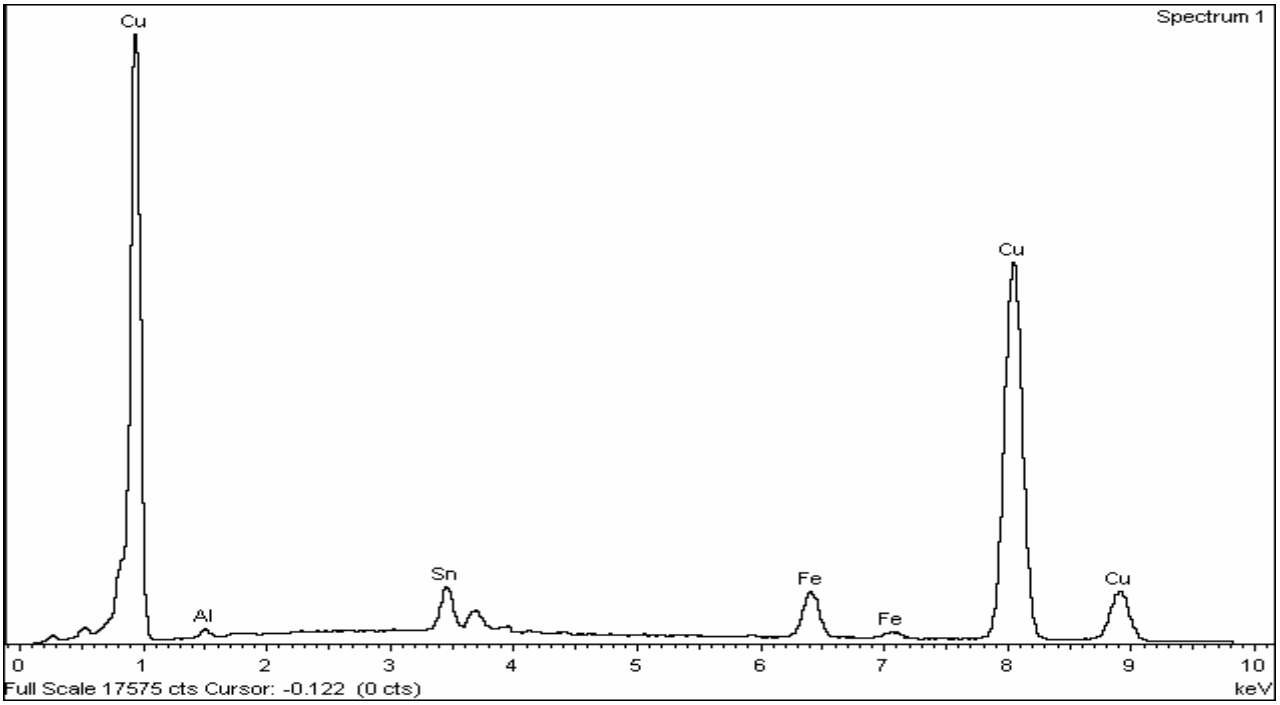

Figure 36: EDS analysis near the fracture surface at Location 1 identified in Figure 35

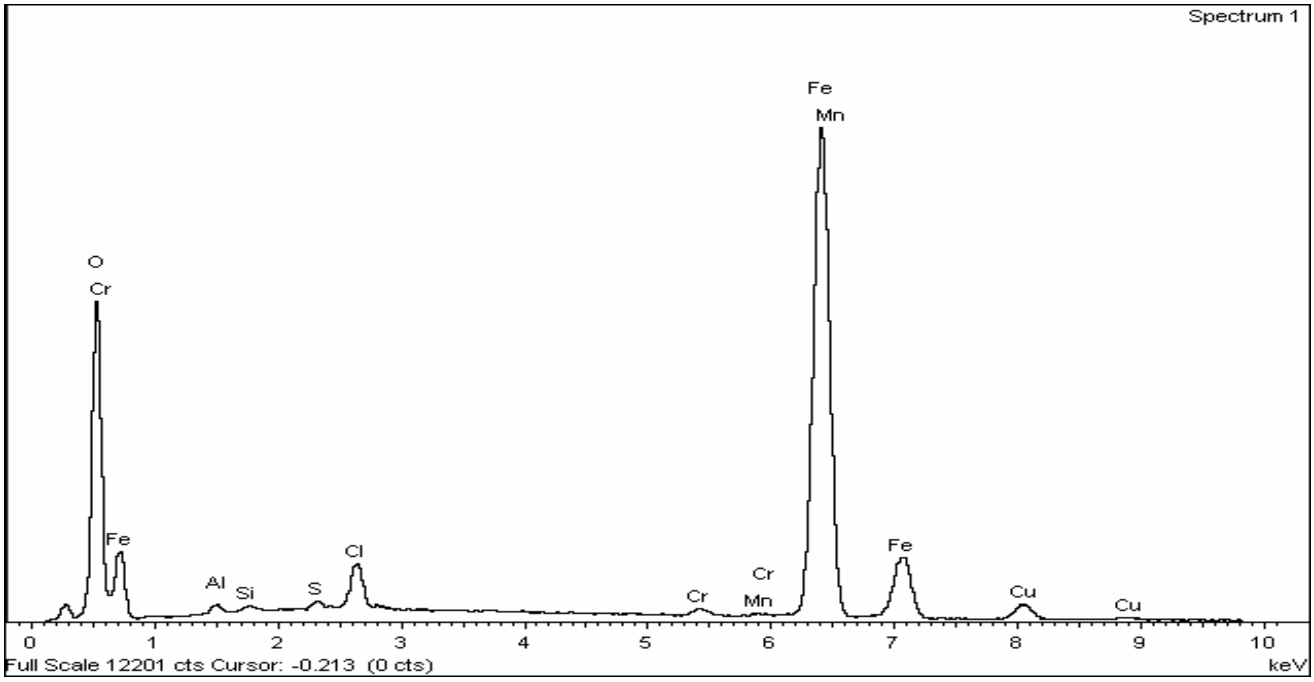

Figure 37: EDS analysis near the fracture surface at Location 2 identified in Figure 35

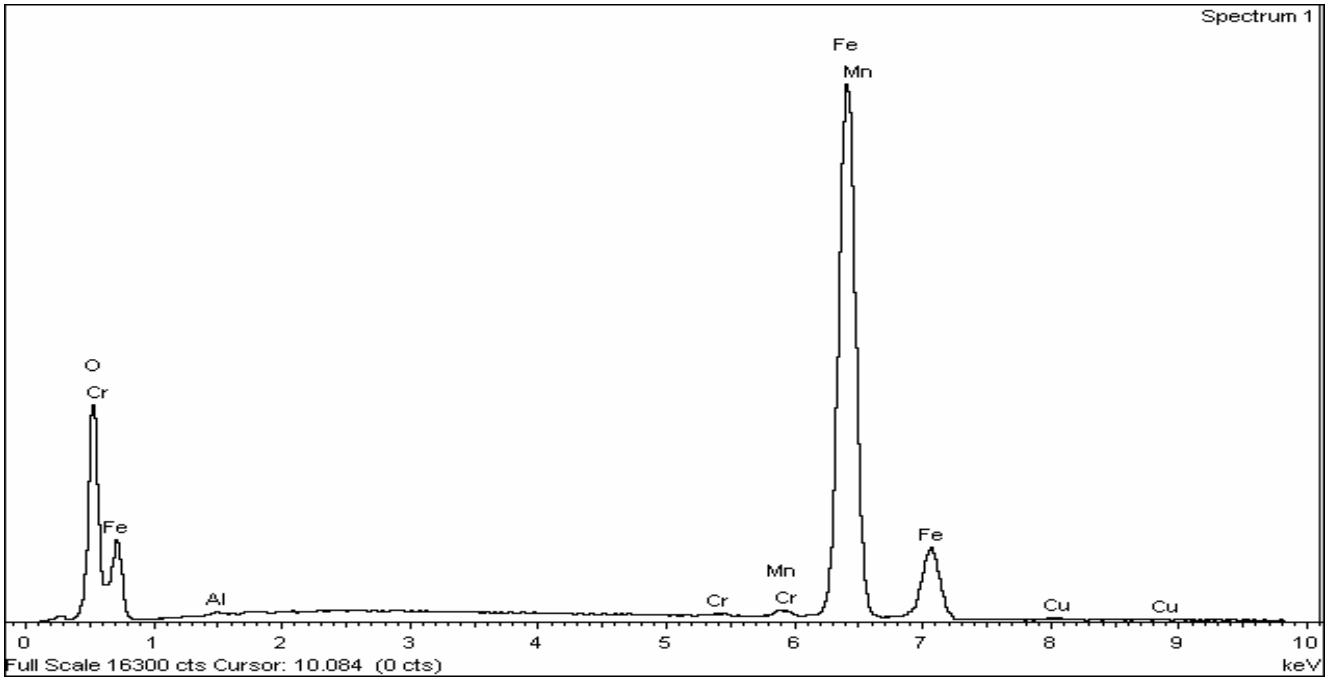

Figure 38: EDS analysis near the fracture surface at location 3 identified in Figure 35

8.0 REFERENCES

1. Code of Federal Regulations (CFR) 49, Chapter I – Research and Special Programs Administration, Department of Transportation, Subchapter C-Hazardous Material Regulations, part § 178.37, pg 729 – 733, 2002.

2. ASM Metals Reference Book, 3rd edition, pg 309, 1993.

3. Heat Treater's Guide Practices and Procedures for Irons and Steels, 2nd edition, Harry Chandler, pg 300, 1995.

4. Metals Handbook, 8th edition, Vol 1, Properties and selection of metals, pg 1027, 1972.

5. Metals handbook, 9th edition, Vol 11, Failure Analysis and Preventions, pg 715 to 727, 1986.